Search for Sleptons at $\sqrt{s} \leq 202$ GeV

PRELIMINARY

DELPHI Collaboration

P. Allport, G. J. Hughes, B. King, S. Martí i García, A. Washbrook
University of Liverpool
M. Berggren, R. Pain, Ph. Schwemling
LPNHE, University of Paris VI & VII, Paris
S. Amato, M. Gandelman, J.H. Lopes
IF-UFRJ, Rio de Janeiro, Brasil
N. Ghodbane
IPNL, University Claude Bernard, Lyon, France

Abstract

Data collected by the DELPHI experiment at centre-of-mass energies from 192 to 202 GeV with an integrated luminosity of 226 pb^{-1} have been used to search for the supersymmetric partners of electrons, muons, and taus in the context of the Minimal Supersymmetric Standard Model. No excess over the expected Standard Model background was found. We present results in terms of exclusion regions in the ($M_{\tilde{\ell}}$,$M_{\tilde{\chi}^0_1}$) planes. For large differences between the slepton and LSP masses, the following 95% CL lower have been set, combining present data with the data collected at lower energies: $M_{\tilde{\mathrm{e}}} \geq 95$ GeV/c^2, $M_{\tilde{\mu}} \geq 86$ GeV/c^2 and $M_{\tilde{\tau}} \geq 74$ GeV/c^2.

Paper submitted to the Moriond 00 QCD and
High Energy Hadronic Interactions Conference
Les Arcs, March 2000

1 Search for Scalar Leptons

In this note we present an update of the search for the supersymmetric partners of the electron, muon and tau leptons, using data collected by DELPHI during 1999 at centre-of-mass energies between 192 GeV and 202 GeV. The analysis was performed on data corresponding to an integrated luminosity of 25.9 pb^{-1} at 192 GeV, 76.8 pb^{-1} at 196 GeV, 82.4 pb^{-1} at 200 GeV and 40.9 pb^{-1} at 202 GeV.

1.1 Search for selectrons and smuons

The event selections were similar to the ones used in the analysis of the data collected at a centre-of-mass energy of 189 GeV. In addition we include results from a complementary analysis based on Neural Networks.

The number of selected candidate smuon and selectron events at each centre-of-mass energy are outlined in Table 1. The number of background events expected from simulated Standard Model processes (principally W-pair production) are also shown.

$\sqrt{s}$	Luminosity (pb^{-1})	Selectrons		Smuons	
		N_{evt} Data	N_{evt} Exp	N_{evt} Data	N_{evt} Exp
192	25.9	6	6.9	2	2.3
196	76.8	31	21.2	6	7.2
200	82.4	19	21.3	3	6.6
202	40.9	12	9.9	2	3.3
Total	226.0	68	59.3	13	20.4

Table 1: Selectron and smuon candidates, together with the total number of background events expected.

Using the selected candidates and the predicted background we derive upper limits on the cross-section for slepton production.

For each point in the slepton-neutralino mass plane we calculate the number of candidates and background that are kinematically compatible with this mass point, together with the efficiency of our selection criteria to a hypothetical signal with these masses.

Thus we derive an upper limit for the production cross-section of a slepton signal at each mass point. By comparing our cross-section limit with the expected SUSY cross-section at that point we can deduce whether this mass combination is excluded by our data.

In calculating the SUSY slepton production cross-sections we have made several assumptions. Firstly, right handed sleptons are expected to have lower masses than the left-handed states. We have therefore made the cautious assumption that only right-handed sleptons are produced and calculated the SUSY cross-section accordingly, assuming the left-handed states to be kinematically inaccessible.

We have calculated the branching ratio of the process $\tilde{\ell} \rightarrow \ell\tilde{\chi}_1^0$, with the SUSY mass parameter, μ, set to -200 GeV/c^2 and with $tan\beta$ set to 1.5. The exclusion limits on $\tilde{e}_R$ and $\tilde{\mu}_R$ production are shown in figures 1 and 2. For large ΔM, the obtained mass limits are $M_{\tilde{e}_R} \geq 95$ GeV/c^2 and $M_{\tilde{\mu}_R} \geq 86$ GeV/c^2. The corresponding expected limits are

$M_{\tilde{e}_R} \geq 94$ GeV/c^2 and $M_{\tilde{\mu}_R} \geq 83$ GeV/c^2. These results have been obtained by combining the data taken during 1999 with that recorded in 1997 and 1998 at centre-of-mass energies from 183 GeV to 189 GeV.

1.1.1 Search for selectrons and smuons with Neural Networks

As a cross-check, an analysis based on a neural network method[1] was developed for the searches for selectrons and smuons in the same data samples. Events were selected by applying the same pre-selection criteria as in the sequential cuts analysis described above.

Since the signal characteristics depends strongly on the difference of masses between the slepton and the neutralino, $\Delta M (= M_{\tilde{\ell}} - M_{\tilde{\chi}^0_1})$, the analysis was divided into three ΔM windows: $\Delta M \leq 10$ GeV/c^2, 10 GeV/$c^2 < \Delta M \leq 30$ GeV/c^2 and $\Delta M \geq 30$ GeV/c^2. The neural structure was trained to recognize signal and background separately in each window. The neural consisted of three layers:

- 13 input nodes : the total and transverse visible energy, three components of the missing momentum and transverse missing momentum (4 variables), the total momentum, the transverse momentum and the polar angle of each lepton (6 variables), the polar angle of the missing momentum, the invariant mass of the event and the invariant mass of the lepton pair.
- 13 hidden nodes.
- 3 output nodes linked to the three kinds of process the neural network should discriminate: the signal, the two photon background (which has a dominant contribution for $\Delta M \leq 10$ GeV/c^2) and the W^+W^- background (dominant for $\Delta M \geq 30$ GeV/c^2).

The same variables were used for the three mass windows and the final cut on the neural network output was then optimized to minimize the expected excluded cross section. The numbers of events in the real data and in the simulated data passing the cuts in any of the three windows are listed in Table 2. The efficiencies for the selectron and the smuon

$\sqrt{s}$	Luminosity (pb^{-1})	Selectrons		Smuons	
		N_{evt} Data	N_{evt} Exp	N_{evt} Data	N_{evt} Exp
192	25.9	4	4.31	1	2.48
196	76.8	6	4.51	6	6.32
200	82.4	6	8.06	4	6.93
202	40.9	3	5.54	2	3.43
Total	226.0	19	22.42	13	19.16

Table 2: Selectron and smuon candidates, together with the total number of background events expected in the Neural Network analysis.

production were computed for several combinations of $M_{\tilde{l}}$ and $M_{\tilde{\chi}^0_1}$ with $M_{\tilde{l}}$ and $M_{\tilde{\chi}^0_1}$ varying with a step of 5 GeV/c^2 and interpolated in between. Exclusion limits on $\tilde{e}_R$ pair-production and on $\tilde{\mu}_R$ pair-production were then obtained for $\mu = -200$, $\tan\beta = 1.5$ taking into account the signal efficiencies, number of candidates and background for each

[1] A.Zell et *al.* `SNNS V 4.1`, Stuttgart neural network simulator, Report number 6/95.

($M_{\tilde{l}}$,$M_{\tilde{\chi}^0_1}$) point. For large ΔM, mass limits could be set at $M_{\tilde{e}_R} \geq 93$ GeV/c^2 and $M_{\tilde{\mu}_R} \geq 85$ GeV/c^2. The expected limits were evaluated to be $M_{\tilde{e}_R} \geq 91$ GeV/c^2 and $M_{\tilde{\mu}_R} \geq 79$ GeV/c^2. Hence, the neural network analysis is slightly less performant than the sequential cuts analysis, but yields similar results.

1.2 Search for staus

The procedure to select stau candidates was similar to the one used in the analysis of the data taken at 189 GeV. Due to the higher energies and higher integrated luminosity expected in 1999, the cuts were re-tuned to obtain an optimal expected exclusion limit at higher masses. This optimization yielded a working-point with higher efficiency but also with higher expected background. The analysis was divided in two regions depending on the mass difference between the stau and the LSP: ΔM larger or smaller than 20 GeV/c^2. The main difference was that in the low ΔM region, candidates with smaller missing transverse momentum were accepted. ($p_T^{\rm miss}$ was requested to be larger than 6 GeV/c as compared to 8 GeV/c in the high ΔM region.) To keep the background from two-photon events at an acceptable level, with the more relaxed cut in the transverse momentum, other cuts were made more stringent.

Table 3 summarizes the number of accepted events in the data for the different selections together with the expected number of events from the different background channels. In both ΔM regions, a slight over-all excess of events was observed: In the high ΔM region a total of 25 candidates were found, with an expected background of 19.2±0.7 . In the low ΔM region, 18 candidates were found, with an expected background of 12.6±0.6 . In the high ΔM region, four-fermion events constitute 68 % of the background, $\gamma\gamma$ events 22 %, and two-fermion events the remaining 10 %. In the low ΔM region, the corresponding fractions are 83 %, 11% and 6%, respectively. Note that a large fraction of the four-fermion events are not kinematically compatible with low ΔM and will not enter into the evaluation of the cross-section limit in that region.

$\sqrt{s}$	Luminosity (pb^{-1})	$\Delta M \geq 20$ GeV/c^2		$\Delta M < 20$ GeV/c^2	
		N_{evt} Data	N_{evt} Exp	N_{evt} Data	N_{evt} Exp
192	25.9	3	1.8 ± 0.2	1	1.8 ± 0.2
196	76.8	8	6.4 ± 0.3	6	4.5 ± 0.4
200	82.4	11	8.0 ± 0.5	8	4.1 ± 0.2
202	40.9	3	3.0 ± 0.3	3	2.4 ± 0.3
Total	226.0	25	19.2 ± 0.7	18	12.6 ± 0.6

Table 3: Stau candidates, together with the total number of background events expected.

Exclusion limits on $\tilde{\tau}\tilde{\tau}$ production were obtained taking into account the signal efficiencies for each mass point, as well as all candidates in the real data and in the simulated background which were kinematically compatible with the mass combination. When determining whether data or background events were kinematically compatible with the mass point, the end point of the expected momentum spectrum of the visible reconstructed τ was used. Figure 3 shows the 95% CL exclusion region in the ($M_{\tilde{\tau}_R}$,$M_{\tilde{\chi}^0_1}$) plane

obtained by combining present data with the data taken at the centre-of-mass energies from 130 to 189 GeV. Figure 4 shows the exclusion region in the case of the minimal mixing. Due to the vanishing coupling to the Z^0 at this mixing angle, no limit can be inferred from the precision measurements at LEP I in this case. The region below $M_{\tilde{\tau}} = 25$ GeV/c^2 does not include the data from 1999. A lower limit on the stau mass can be set at 74 to 75.5 GeV/c^2 (depending on the mixing) if the neutralino mass is below 60 GeV/c^2 and the mass differences between the stau and the LSP above is 6 GeV/c^2. The expected limit is between 77 and 79 GeV/c^2.

2 Conclusions

In a data sample of 226 pb^{-1} collected by the DELPHI detector at centre-of-mass energies ranging from 192 to 202 GeV, searches were performed for the selectron, smuon and stau production.

For the selectron search, good agreement was found with the Standard Model prediction, and by combining the present data with the data collected at centre-of-mass energies from 183 GeV to 189 GeV, a mass limit for $\tilde{e}_R$ can be set at 95 GeV/c^2 for large ΔM.

In the search for smuon production, the number of candidates seen in the data agrees well with the expected Standard Model background. Combining this data with the lower energy data, a mass limit for $\tilde{\mu}_R$ can be set at 86 GeV/c^2 for large ΔM.

In the search for stau production, we also find agreement with the expectation from the Standard Model. Combining present data with the data collected at centre-of-mass energies between 130 and 189 GeV, a mass limit for the stau can be set at 75.5 GeV/c^2 if the stau is purely a partner to the right-handed τ. In the case where the stau mixing angle is such that the production cross-section is at a minimum, the mass limit is 74 GeV/c^2. These limits are valid if the LSP mass is below 60 GeV/c^2 and the mass difference between the stau and the LSP is above 6 GeV/c^2.

Acknowledgments

We express our gratitude to the members of the CERN accelerator divisions and compliment them on the fast and efficient commissioning and operation of the LEP accelerator in this new energy regime.

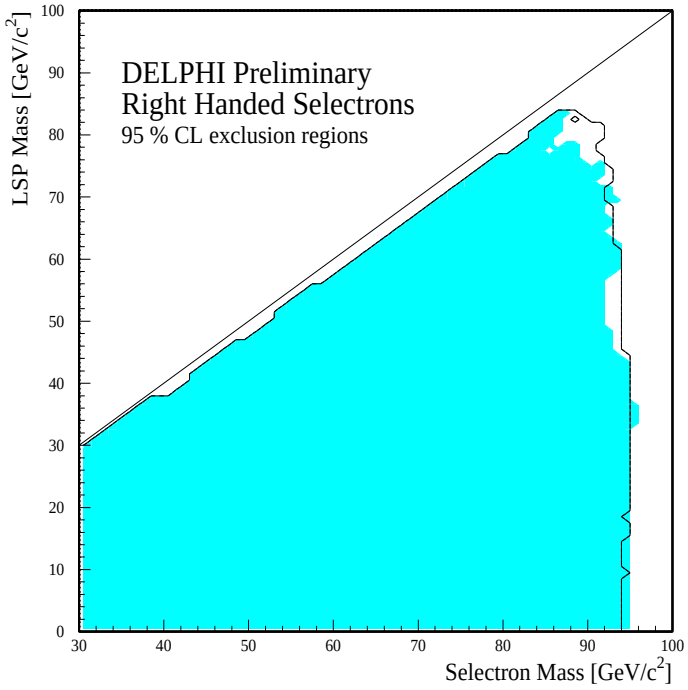

Figure 1: 95% CL exclusion region in the ($M_{\tilde{e}_R}$,$M_{\tilde{\chi}^0_1}$) plane. The shaded region shows the obtained exclusion limit, and the solid line shows the limit expected for no signal events.

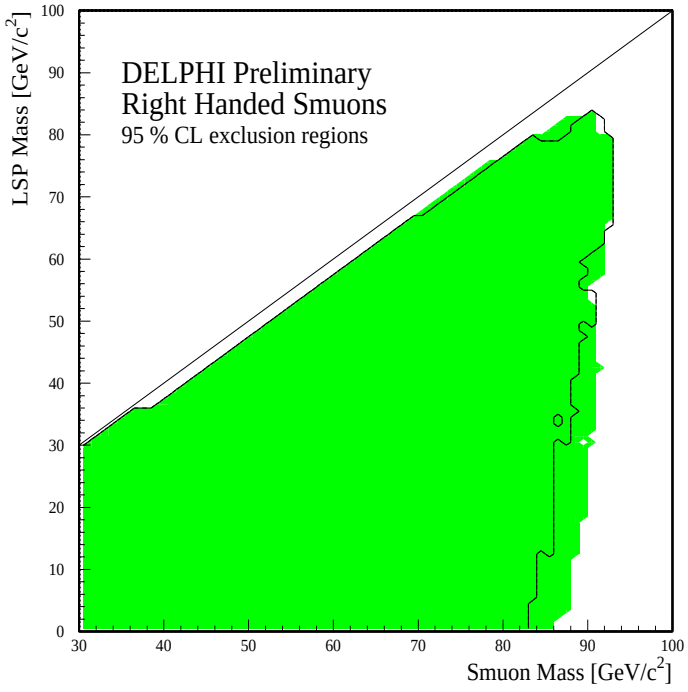

Figure 2: 95% CL exclusion region in the ($M_{\tilde{\mu}_R}$,$M_{\tilde{\chi}^0_1}$) plane. The shaded region shows the obtained exclusion limit, and the solid line shows the limit expected for no signal events.

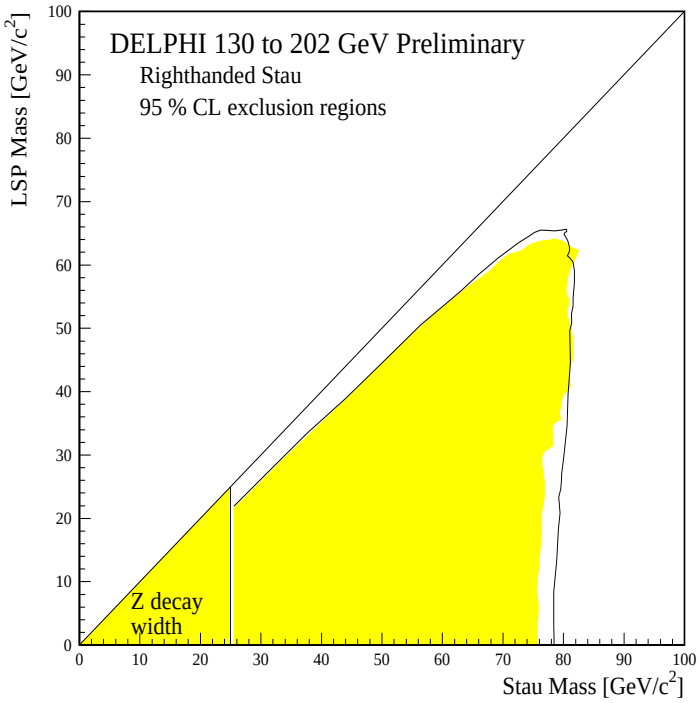

Figure 3: 95% CL exclusion region in the ($M_{\tilde{\tau}_R}$,$M_{\tilde{\chi}_1^0}$) plane. The shaded region shows the obtained exclusion limit, and the solid line shows the limit expected for no signal events.

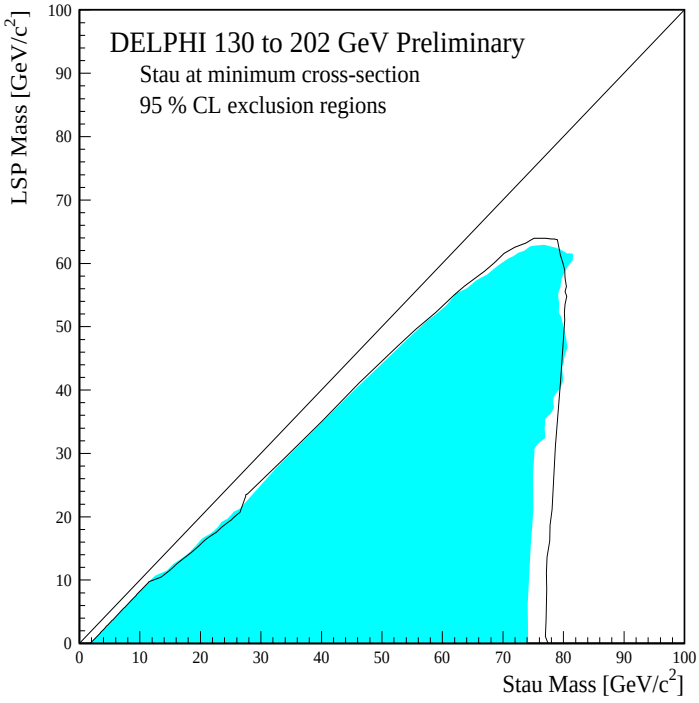

Figure 4: 95% CL exclusion region in the ($M_{\tilde{\tau}}$,$M_{\tilde{\chi}_1^0}$) plane obtained for the minimal $\tilde{\tau}$ pair-production cross-section. The shaded region shows the obtained exclusion limit, and the solid line shows the limit expected for no signal events.